



HAL
open science

Simultispin: A versatile graphical user interface for the simulation of solid-state continuous wave EPR spectra

Florian Molton

► **To cite this version:**

Florian Molton. Simultispin: A versatile graphical user interface for the simulation of solid-state continuous wave EPR spectra. *Magnetic Resonance in Chemistry*, 2020, 58 (8), pp.718-726. 10.1002/mrc.5019 . hal-04643478

HAL Id: hal-04643478

<https://hal.science/hal-04643478v1>

Submitted on 10 Jul 2024

HAL is a multi-disciplinary open access archive for the deposit and dissemination of scientific research documents, whether they are published or not. The documents may come from teaching and research institutions in France or abroad, or from public or private research centers.

L'archive ouverte pluridisciplinaire **HAL**, est destinée au dépôt et à la diffusion de documents scientifiques de niveau recherche, publiés ou non, émanant des établissements d'enseignement et de recherche français ou étrangers, des laboratoires publics ou privés.



Simultispin: a versatile graphical user interface for the simulation of solid-state continuous-wave EPR spectra

Journal:	<i>Magnetic Resonance in Chemistry</i>
Manuscript ID	MRC-19-0171.R1
Wiley - Manuscript type:	Research Article
Date Submitted by the Author:	n/a
Complete List of Authors:	Molton, Florian; Univ. Grenoble Alpes, UMR CNRS 5250, Département de Chimie Moléculaire
Keywords:	EPR, Easyspin, Simulation, Graphical user interface, Transition metal complexes

SCHOLARONE™
Manuscripts

Simultispin: a versatile graphical user interface for the simulation of solid-state continuous-wave EPR spectra

Florian Molton^{a,*}

^a *Univ. Grenoble Alpes, UMR CNRS 5250, Département de Chimie Moléculaire, 38000 Grenoble, France.*

Corresponding author: florian.molton@univ-grenoble-alpes.fr

Abstract

Solid-state continuous wave (cw) electronic paramagnetic resonance (EPR) spectroscopy is particularly suitable for metal complex analysis. Extracting magnetic parameters by simulation is often necessary to describe the electronic structure of the studied molecular compounds that can have various electronic spin states and characterized by different parameters like g-values, hyperfine coupling or zero field splitting values. Easyspin toolbox on Matlab is a powerful tool but for the user, it requires spending time with coding, and could discourage non-experts. Face to this context, we have developed a graphical user interface called Simultispin, dedicated to solid-state cw-EPR spectra simulation. Some examples of experimental spectra of metal complexes (mixture of low spin and high spin Fe^{III} complexes, dynamic disorder of a Cu^{II} complex, photogeneration of a Mn^{III} complex), highlighting specific solid-state functions, are described and analyzed based on simulations performed with Simultispin. We hope that its ergonomics and the ease to set up a complete set of parameters to get reliable simulations could help a large EPR community to improve the efficiency of their interpretations.

Introduction

Electron Paramagnetic Resonance (EPR) spectroscopy targets unpaired electrons, dedicating this technique to paramagnetic species mainly composed of organic radicals and/or transition metals. EPR is a tool of interest for a wide range of applications: from biology with protein mobility or detection of reactive oxygen species to material structures, radio dosimetry and many more.^{[1]-[3]} In the specific case of metal complexes, for which experiments are mainly carried out at low temperature in frozen solution or in powder, continuous wave (cw) EPR analysis help to investigate the electronic properties such as oxidation state and spin state, electronic structure or magnetic temperature dependence.^{[4]-[6]} Simulating is essential to have access to magnetic parameters as they need to be extracted from the experimental spectra in order to sustain interpretations and confirm (or not) hypothesis. Because of the variety of transition metal compounds and their electronic properties (electronic spin, orbital splitting, anisotropy, ...),^[7] the simulation process requires a versatile tool able to deal with these multiple requests. The XSophe commercial Bruker package can perform solid-state spectra simulations. However, this software is expensive, difficult to use and only works under Linux system. Regarding Simfonia, it is out of date. Currently, the most widespread, updated and free of charge alternative to simulate is the powerful EPR toolbox on Matlab called Easyspin.^[8] It offers the possibility to simulate and fit almost all kind of imaginable spectra with a great set of functions including slow motion, fast motion and solid-state. The use of Easyspin for non-expert requires time to learn how to code with Matlab and how to deal with an abundance of parameter options. One solution is the use of a Graphical User Interface (GUI) to make the experience more ergonomic. The calculation process is still managed by the Easyspin program and the GUI facilitates the interaction between the user and the computing system with a selection of practical tools and pertinent parameters. Simlabel GUI is an efficient add-on but it focuses on slow motion and spin labelling.^[9] Even if a solid-state mode is available, parameters are restricted to systems with an electronic spin state of $S = 1/2$.

Here we present a new GUI, called Simultispin, particularly dedicated to transition metal EPR spectra. It is based on the Simlabel code, thus using its form and practical tools but the background has been fully rethinking to answer solid-state simulation problematic. This is reflected in new major settings including the electronic spin state not

limited to 1/2 adapted for high spin and polynuclear compounds and the magnetic anisotropy, i.e. the Zero Field Splitting (ZFS) described by the D and E parameters for $S > 1/2$. Strain option could be set for anisotropic broadening, as well as the parallel mode of the magnetic field modulation appropriate for integer electronic spins. Concerning the experimental spectra, the temperature at which they have been recorded can be set and a baseline correction tool has been implemented. The ability to load, save and compare both experimental and simulated spectra is still available as well as the multi-component windows and the fitting mode. The most significant characteristics of Simultispin will be further discussed with some experimental examples.

System requirements

Matlab 7.5 or later version needs to be installed on a standard computer with either Windows, Linux or Mac OS. The Easyspin toolbox can be downloaded online at <http://easyspin.org/download.html> and needs to be set on Matlab. Simultispin package is available online for free at <http://easyspin.org/forum/> under the section « Easyspin file exchange » or on the GitHub platform. The forum post section is open for user feedbacks and a user guide is provided in the package for getting started.

Please cite Easyspin^[8] and this paper in any publications using Simultispin.

Overview of the main panel

Simultispin is composed of two different windows: the main panel (Figure 1) and the parameter component panel (Figure 3).

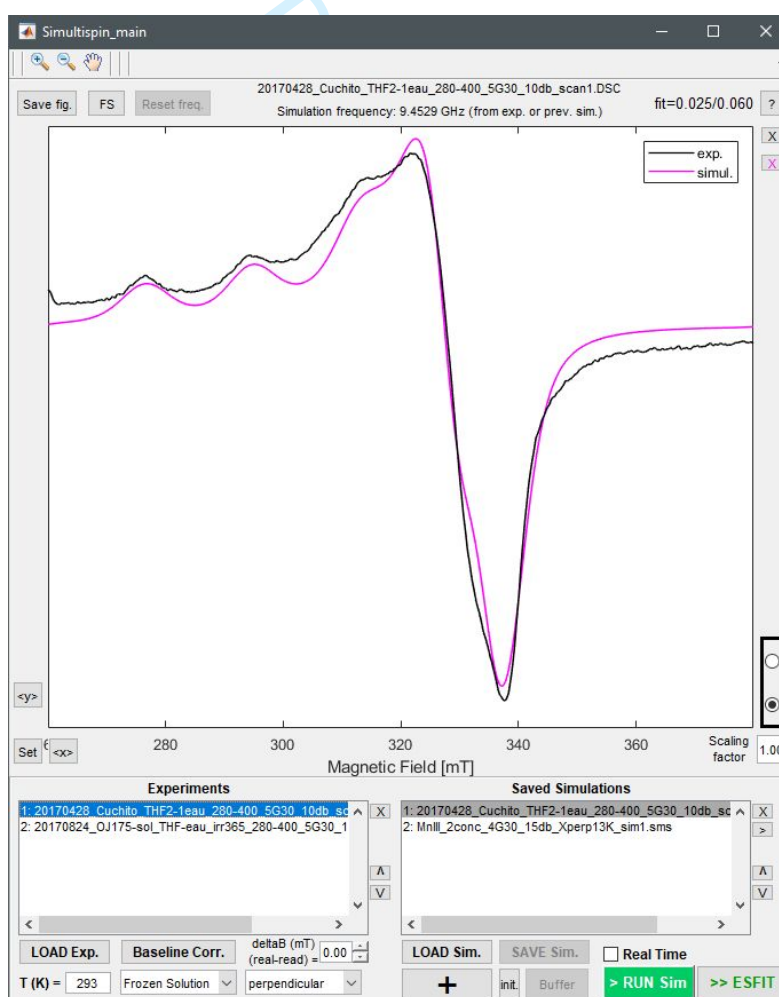


Figure 1: Screen shot of the main panel of Simultispin. Example with the X-band cw-EPR spectrum of a Cu^{II} complex in powder at room temperature. Experiment in black, simulation in pink.

The upper part of the main panel (Figure 1) is the graph figure plotting spectra with usual buttons to adapt the view (zoom in/out, full scale, hand, x and y scaling, normalization). The lower part of the main panel includes the list of experimental and simulated spectra associated with buttons to load, save, remove and reorganize the files. The experimental parameters that can be set up are the temperature (100 K by default), the magnetic field shift and the magnetic field modulation mode. The perpendicular mode is the default one for common cw-EPR, whereas the parallel one is often used to detect non-Kramers transitions arising from samples with integer electronic spin state.^[10] The last parameter of simulation available on the main panel is the simulating function. Actually, Easyspin provides various specific simulating functions adapted to the sample state. In Simultispin, we have decided to retain the « Pepper » function by default dedicated to solid-state (glass, powder or frozen solution) and a secondary « Garlic » function is available in the popup menu for fast motion, typically solution at room temperature. As pre-treatment tool specially developed for Simultispin, a baseline correction option is accessible with a button from the main panel (Figure 2). When one experimental spectrum is selected, the user is invited to select abscissa of points with a crosshairs directly on the graph. Then the program calculates and plots a baseline fit built with the Matlab spline function. This process can be repeated until the user is satisfied and the corrected spectrum can be saved in BES3T Bruker format, including the experimental frequency, for further analysis and simulation.

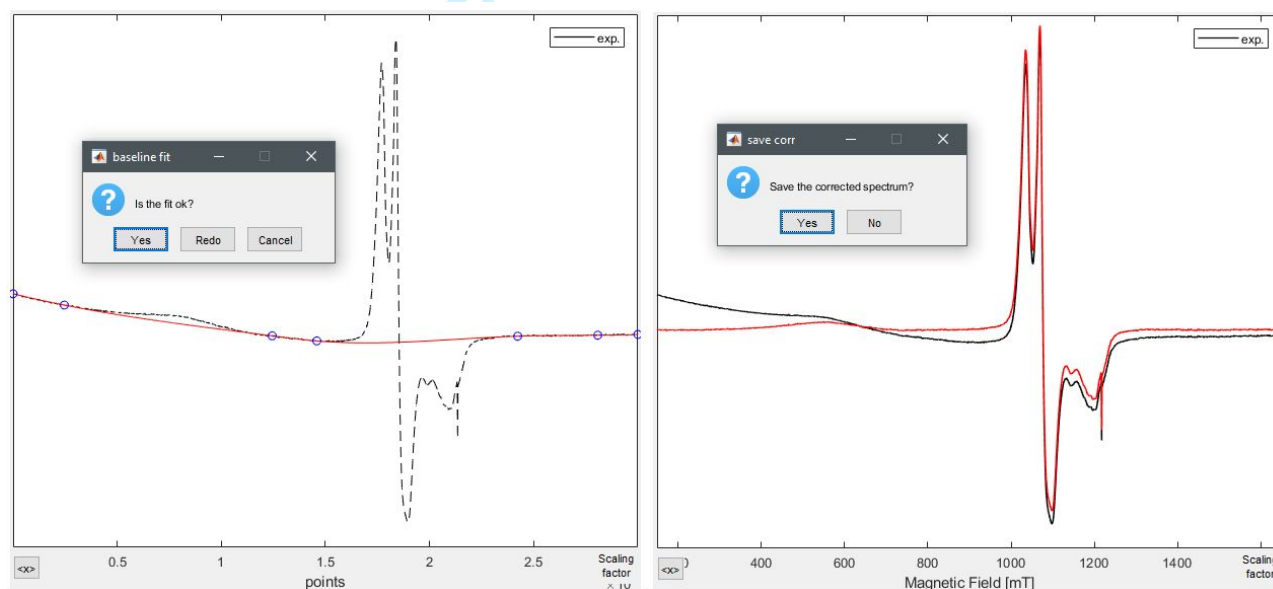


Figure 2: Screen shots during the baseline correction process. Left graph shows the baseline fit (in red) calculating after having chosen some points abscissa (blue circles). Right graph shows the corrected spectrum in red, compare to the raw spectrum in black.

The « + » button creates an additional parameter component window, which is described in the following section. This latter is linked to additional options (« init. » to set the initial default parameter values and « buffer » to return to the last unsaved parameters). Finally, the last buttons come for « run » the simulation by processing the whole input parameters and run the « ESFIT » fitting mode. Notice that at the top right of the main panel a help button refers to an explicit user guide.

Overview of the parameter component window

From general settings, we now move to individual species parameters by opening the component window (Figure 3). It allows describing finely the sample. In the case of a mixture, several component windows can be open with independent settings for each of them. Their relative weight can be notified and will be taken into account for the simulation. For each window, the name of the compound can be edited. The input spin variables to be set are the electronic spin (by step of 1/2), the isotropic line width (gaussian or lorentzian shape or mixture), *g-values* (isotropic, axial or rhombic), two hyperfine coupling sets A₁ and A₂ with popup menu to choose the nuclear spin value up

to $7/2$, some strain settings ($HStrain$, $gStrain$ and $AStrain$) to refine anisotropic linewidth and finally the zero field splitting D and E parameters for $S > 1/2$. For these latter, a specific help button opens a documentation including rhombograms for $S = 3/2$ and $5/2$.^[11] Note that g_{iso} , A_{iso} and E/D values are automatically calculated from the inputs.

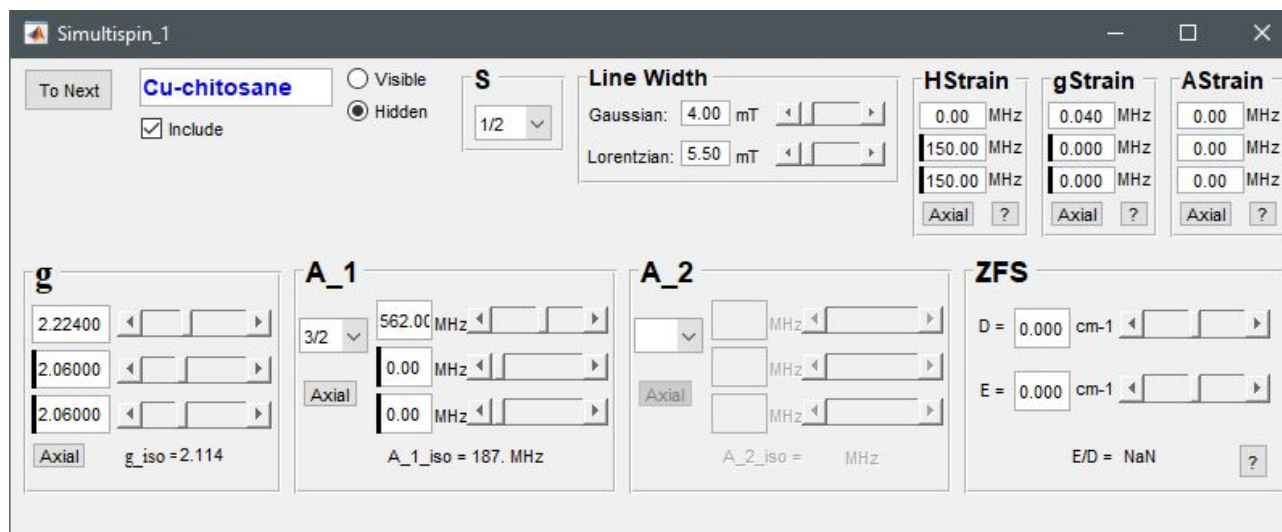


Figure 3: Screen shot of the first component window for the Cu^{II} complex spectrum in powder shown in Figure 1. Black markers represent the chosen axiality for g -values, hyperfine coupling and strains. They can be set according to the system by clicking on the "Axial" buttons.

Once parameters have been set, the « Run Sim. » button processes the calculation, thus the resulting simulated spectra is plotted on the figure of the main panel. It has to be highlighted that Simultispin automatically picks up the frequency from the selected experimental spectrum (Bruker file) of the list but if no experiment has been chosen, the frequency should be set manually. From this starting point, the user is then free to modify each parameter and to reprocess the simulation. One convenient option is to tick the « real time » mode on the main panel, which allows visualizing in direct the effect of one by one parameter change.

To keep the interface light and easy to use, only a bunch of parameters has been implemented. A large panel of spectra can still be simulated with this selection. However, for more complicated systems which need additional parameters, the only way is to code directly on Matlab with the appropriate Easyspin functions.

Fitting process and comparison feature

After saving the parameters of the simulation, the fitting mode could be processed with the « ESFIT » button. A table opens with all the parameters of the simulation and their auto varying range to select. The amplitude of variation can also be manually edited. After selection, the dedicated least-squares fitting GUI, directly implemented from Easyspin, will pop up to manage the fitting process. Among several options not described here,^[12] the best parameters found during the fitting process can be exported and saved as a new simulated spectrum. Thus, they will be automatically copied and displayed in the parameter component windows for further treatments. The user has to pay attention that the fitting process could be a source of spectroscopic nonsense. The more numerous the selected parameters are, the higher the risk is to find a combination which does not have any scientific rational. It is advised to analyze first the system, then to simulate it as fine as possible before to run the fitting process with only one or two "free" sets of parameters.

One strength of Simultispin is its ability to open and compare several spectra, either experimental or simulated, one by one or together. For a multi component spectrum, the contribution of each species can be selected individually to be compared with the full spectrum to help the analysis. This flexibility offers more efficiency for the workflow and fosters a step back on the multiple data. Exportation is another time saving feature by saving the current figure as a picture (button « FS » at the top left of the main panel) or by exporting experimental and

simulated data together in a multiple-column ASCII file in addition to a parameter file (button « > » of the simulated spectra list).

The functionality of Simultispin and its behavior toward various solid-state metal spectra is described next with some concrete examples.

Fe^{III}-OOH intermediates in H₂O₂ catalytic oxidation^[13]

In the topic of bio-inorganic enzymes and their biomimetic analogues, the Fe^{IV}=O units have been intensively studied over the past decade as they play an active role in the oxidation of organic substrates by enzymes. Its formation via homolytic O-O bond cleavage of the corresponding Fe^{III}-OOH complex has been demonstrated when high spin species are concerned, whereas such a process was still not observed from low spin Fe^{III}-OOH species. In this context, EPR spectroscopy was used in combination with UV-Vis spectroscopy monitoring to better understand the oxidation mechanism of [(N4Py)Fe^{II}(OCH₃)₂]²⁺ complex **(1)** (N4Py = 1,1-bis(pyridin-2-yl)-*N,N*-bis(pyridin-2-ylmethyl)methanamine) into [(N4Py)Fe^{IV}(O)]²⁺ in the presence of H₂O₂ in methanol. The study focused on the involved intermediates [(N4Py)Fe^{III}(OOH)]²⁺ **(2)**, [(N4Py)Fe^{III}(OCH₃)₂]²⁺ **(3)** and [(N4Py)Fe^{III}(OH)]²⁺ **(4)**.

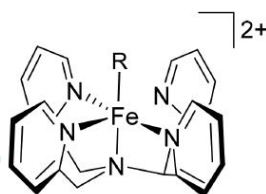


Figure 4: Structure of the complexes. For **(1)** et **(3)** R = O(CH₃), for **(2)** R = OOH, for **(4)** R = OH.

A large excess of H₂O₂ (> 40 eq.) was added to 1 mM of complex **(1)** in methanol. At different times of reaction, aliquots were transferred to EPR tubes and immediately frozen at 77 K.

The experimental X-band cw-EPR spectra after 1.7 min and 127 min of reaction at 32 K (Figure 5a and Figure S1) exhibit peaks in two distinct magnetic field regions. The peak at half field with no hyperfine coupling can be attributed to a high spin $S = 5/2$ Fe³⁺ complex. The effective *g*-value around 4.3 is explained by ZFS interaction with a large magnitude: $D = 2.67$ cm⁻¹ and $E/D = 0.32$. To have been previously described, these parameters are consistent with the signature of **(4)**.^[14]

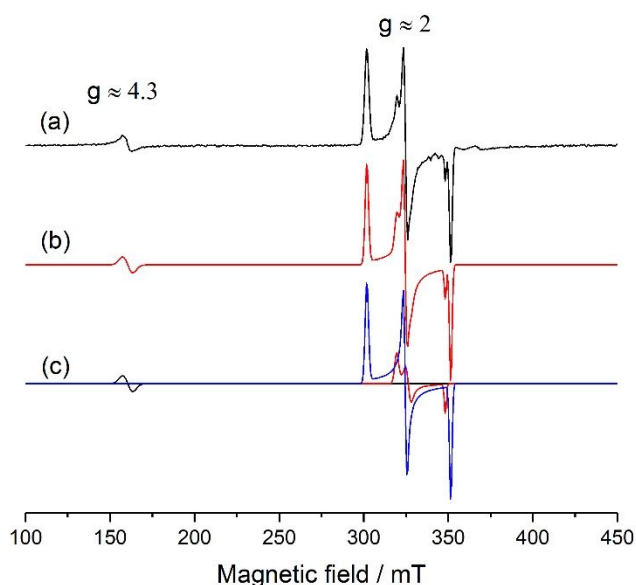


Figure 5: X-band cw-EPR spectra obtained from 1 mM of [(N4Py)Fe^{II}(OCH₃)₂]²⁺ in methanol with a large H₂O₂ excess recorded at 32 K. (a) Experimental spectrum after 127 min, (b) simulated spectrum from Simultispin, (c) simulated spectra of each distinct

component from Simultispin: high spin $[(N4Py)Fe^{III}(OH)]^{2+}$ (**4**) in black, low spin $[(N4Py)Fe^{III}(OOH)]^{2+}$ (**2**) in red and $[(N4Py)Fe^{III}(OCH_3)]^{2+}$ (**3**) in blue.

The combination of peaks with anisotropic shape at g around 2 makes supposed to a mixture of two low spin $S = 1/2$ Fe^{3+} complexes. It is confirmed by simulation with rhombic g-values of [2.155 2.109 1.977] and [2.281 2.121 1.959] characteristic to respectively $Fe^{III}(OOH)$ complex^[15] and $Fe^{III}(OCH_3)$ complex.^[16]

The multi-component windows and the fitting mode of Simultispin have facilitated the task to determine the relative weight of each compound to refine the final simulation (Figure 5b). With time, (**2**) decomposes to form (**3**), which becomes clearly predominant (85%) and a small quantity of (**4**) appears (2%). Indeed, it was shown that in methanol, a large excess of H_2O_2 leads to a competitive disproportionation reaction, forming (**3**) from (**2**), and further (**4**) in case of hydrolyzation.

At the end, by selecting the visibility of each of the three components, their individual contribution can be visualized directly on the GUI (Figure 5c).

All the parameters obtained using the Simultispin GUI are summarized in Table 1.

	S	g	Lw (mT)	HStrain (MHz)	ZFS	Relative weight (%)	
						After 1.7 min	After 127 min
$[(N4Py)Fe^{III}(OH)]^{2+}$	5/2	[2 2 2]	[6 0]	/	$D = 2.67 \text{ cm}^{-1}$ $E/D = 0.32$	0.4	2.2
$[(N4Py)Fe^{III}(OOH)]^{2+}$	1/2	[2.155 2.109 1.977]	[1.3 0]	[70 80 1]	/	39.1	12.3
$[(N4Py)Fe^{III}(OCH_3)]^{2+}$	1/2	[2.281 2.121 1.959]	[1.3 0]	[60 45 30]	/	60.5	85.5

Table 1: X-band EPR parameters calculated from Simultispin simulation for $[(N4Py)Fe^{III}(R)]^{2+}$ complexes in methanol.

Photogeneration of a Mn^{III} complex^[17]

Molecular systems based on Mn^{II} ion complexes are developed in order to achieve the conversion of solar energy to chemical or electrical energy through an oxygen activation process. New Mn^{II} photo-sensitizers with calixarene ligands have been synthesized and studied. $K[(ThiaSO_2)_2(Mn^{II})_4F]$ (**5**) and $[(ThiaSO_2)(Mn^{II})_2(DMF)_4(H_2O)_2]$ (**6**), with $ThiaSO_2 = p$ -tert-butylsulfonylcalixarene playing the role of antenna for the photo-sensitization of the Mn^{II} ion, display a strong luminescence, excited at 350 nm with emission at approximately 600 nm. The irradiation of both complexes in solid state leads to the oxidized $Na[(ThiaSO_2)(Mn^{III})(DMF)_2]$ complex, which has been isolated and characterized by EPR, X-ray and UV-Vis spectroscopies.

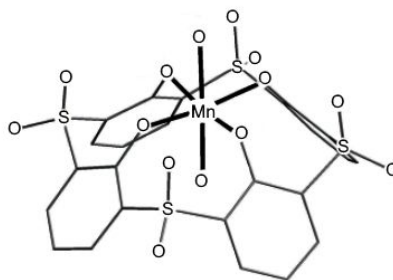


Figure 6: Representation of the octahedral coordination of Mn^{3+} after irradiation of either (**5**) or (**6**)

X-band cw-EPR measurements have been carried out in parallel mode, at 11 K, on the resulting powder obtained after irradiation of either (**5**) or (**6**), in presence of oxygen. The corresponding spectra exhibit a 6-line hyperfine coupling feature at low field (Figure 7, left part).

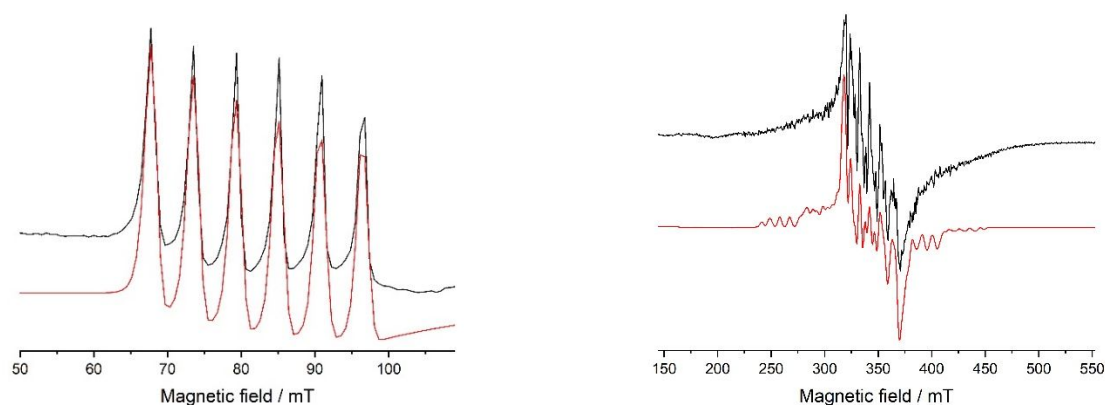


Figure 7: X-band cw-EPR spectrum of $\text{Na}[(\text{ThiaSO}_2)(\text{Mn}^{\text{III}})(\text{DMF})_2]$ in powder at 11 K. left graph is recorded in parallel mode, right graph is recorded in perpendicular mode. Experimental spectra in black, simulations in red.

Parameters extracted by simulation with Simultispin are concordant with a Mn^{III} complex: $S = 2$, $g = [2.1990 \ 1.985]$, $I^{55}_{\text{Mn}} = 5/2$ with $A = [172.8 \ 162.8 \ 159.1]$ (MHz), $H_{\text{strain}} = [1800 \ 1800 \ 0]$ (MHz), $D = 2.17 \text{ cm}^{-1}$ and $E/D = 0.11$. This result confirms the oxidation of the initial Mn^{II} complex by photo-activation. In perpendicular mode, we still observed the characteristic signal of the Mn^{II} ion arising from the initial compound (Figure 7, right part), meaning that only a part of the Mn^{II} complex was oxidized to Mn^{III} .

Dynamic Jahn-Teller effect of a Cu^{II} complex^[18]

In the case of complexes with partial occupancy of their e_g orbitals (typically octahedral copper(II) complexes), the Jahn-Teller theory predicts that the degeneracy of the 2E_g ground state will be splitted. This is traduced by either a compression or rather preferably an elongation of the Cu-ligand bonds parallel to one of the three molecular axes of the complex. Usually the detection of this phenomenon can easily be detected by measuring the variations of the metal-ligand distances by X-ray crystallography. Unfortunately, sometimes X-ray structures does not raise the doubt about any distortions, masking static or dynamic disorder. Thus, EPR spectroscopy becomes a tool of choice as the two occupying configurations for the unpaired electron in the ${}^3d_{x^2-y^2}$ or ${}^3d_z^2$ orbital generate different EPR spectra. This situation happened in the study of the mononuclear octahedral Cu^{II} complex $[\text{Cu}(\text{bmet})](\text{ClO}_4)$ (with $\text{bmet} = N,N'$ -bis(2,2'-bipyridin-6-ylmethyl)ethane-1,2-diamine)).

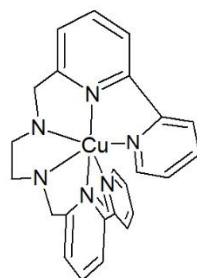


Figure 8: Structure of the complex $[\text{Cu}(\text{bmet})]^+$.

Its careful X-ray characterization revealed a possible masked disorder of an elongated Jahn-Teller axis that was investigated by EPR spectroscopy. Q-band EPR spectra recorded on powder at different temperatures, clearly show a change in the electronic ground state between 20 K and 298 K (Figure 9).

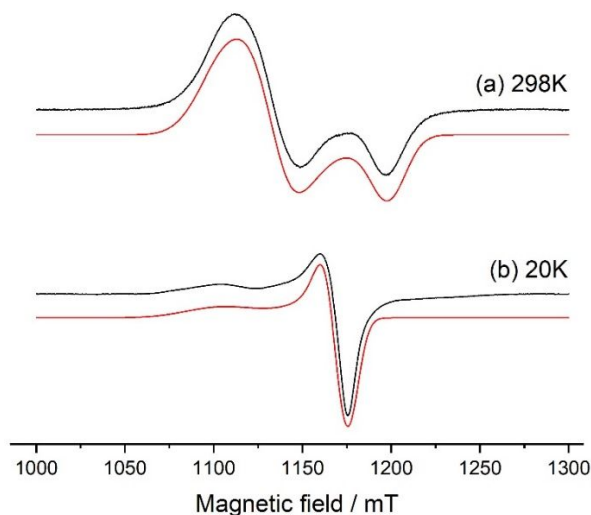


Figure 9: Q-band cw-EPR spectra of $[\text{Cu}(\text{bmet})](\text{ClO}_4)$ as a powder recorded at (a) 298 K and (b) 20 K. Experimental spectra in black, simulations in red.

Indeed at the low temperature, the EPR spectrum displays a quasi-axial Cu^{II} signal with $g_1 > g_2 \geq g_3 > g_e$, whereas at room temperature the spectrum pattern is more rhombic with $g_1 \geq g_2 > g_3 > g_e$ (Table 2).^[19] By using the comparison mode of Simultispin, both simulated spectra can be overlaid and a table summarizes the parameters. This tool helps to clarify the view of these structure changes (Figure 10).

Combined with Density Functional Theory calculations, this result evidences that the rigidity of the bmet ligand along the tetragonal axis is contrary to the Jahn-Teller effect and is at the origin of the rhombic signal recorded at room temperature. In spite of this apparent tetragonal compression of the complex at higher temperature, the dissymmetry of the ligand leads to an octahedron, which is tetragonally elongated at lower temperature, producing the quasi-axial signal observed. This phenomenon is due to a so-called pseudo Jahn-Teller effect.

	S	T (K)	g	Lw (mT)	$HStrain$ (MHz)
$[\text{Cu}^{\text{II}}(\text{bmet})](\text{ClO}_4)$	1/2	298	[2.196 2.144 2.027]	[17 0]	[901 632 439]
	1/2	20	[2.211 2.086 2.068]	[12 0]	[1314 100 100]

Table 2: Q-band EPR parameters calculated from Simultispin simulations for the $[\text{Cu}(\text{bmet})](\text{ClO}_4)$ powder.

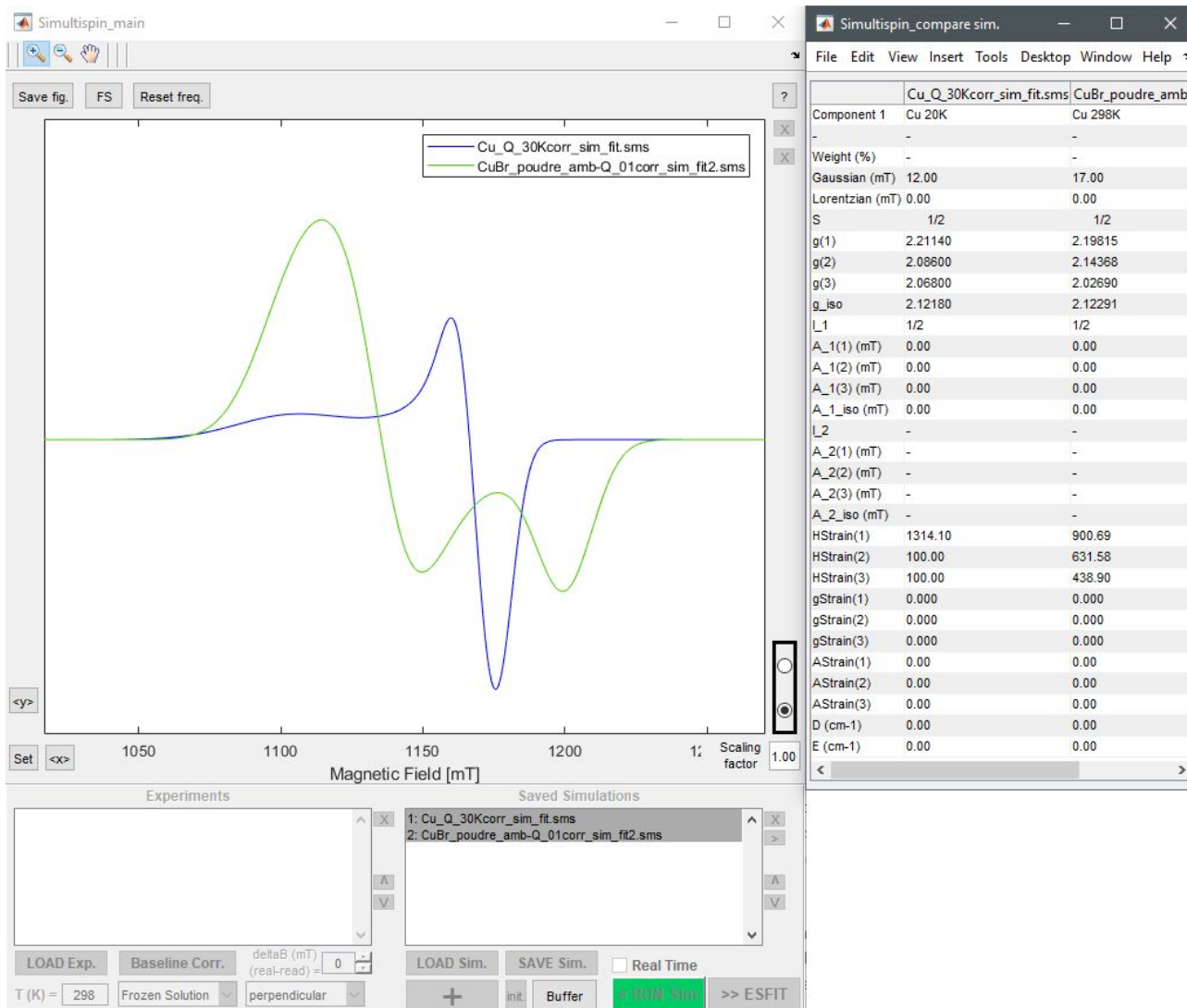


Figure 10: screen shot of the comparison mode of Simultispin for simulated spectra. By selecting several simulated spectra in the list, they are overlaid on the figure and their parameters are compared one by one in a table.

Conclusion

From these experimental applications scanning a variety of metal samples, we have shown how Simultispin meets the need of reliable simulations regardless the complexity of the experimental spectrum. Besides, magnetic anisotropy, multi component weights, high frequency and parallel mode have been investigated in these examples. This GUI is dedicated to solid-state samples and particularly for metal complexes. In that way, the user is not limited to $S = 1/2$. In addition, two hyperfine coupling systems as well as strain effects for anisotropy can be set. A baseline correction tool has been created and some features to import / export, compare and overlay either experimental or simulated spectra are also available. A new feature of kinetic directly included in the GUI, consisting of a double integration tool of the signal for a batch of spectra, is under way. We hope that users, experts as well as non-specialists with Easyspin, could find in Simultispin an efficient and user-friendly interface for their EPR simulations and fittings.

Experimental section

X-band EPR spectra were recorded at helium temperature with an EMX Bruker spectrometer equipped with an ER4116DM Bruker cavity, an ESR900 continuous-flow Oxford Instrument cryostat and an ER4131VT Bruker temperature controller. All spectra presented were recorded under non-saturating conditions.

Q-band EPR spectra were recorded with an EMX Bruker spectrometer equipped a ER5106 Bruker cavity and with the same temperature devices as for X-band EPR experiments.

1 EPR spectral simulations were carried out using Easyspin toolbox on Matlab interfaced with Simultispin GUI.
2
3

4 **Acknowledgements**

5 We are grateful to the IR-RPE CNRS FR3443 RENARD network for EPR facilities. We thanks the authors of the
6 examples cited in this article (Wesley R. Browne, Cédric Desroches and Allan G. Blackman) to have allowed the
7 partial transcription of their results. We are grateful to E. Etienne to share the code of his Simlabel GUI and to C.
8 Duboc for her daily advices.
9

10 **References**

- 11
12
13 [1] D. V. Avila and A. G. Davies, *J. Chem. Soc. Faraday Trans.*, **1990**, 86, 19, 3243–3246.
14 [2] V. Guilarte, F. Trompier, and M. Duval, *PLoS One*, **2016**, 11, 3.
15 [3] J. P. Klare, *Biological Chemistry*. 2013.
16 [4] A. Lannes *et al.*, *J. Am. Chem. Soc.*, **2016**, 138, 50, 16493–16501.
17 [5] M. Xémard *et al.*, *Angew. Chemie - Int. Ed.*, **2017**, 56, 15, 4266–4271.
18 [6] R. Beniazza *et al.*, *Chem. Commun.*, **2015**, 51, 46, 9571–9574.
19 [7] S. Stoll, in *Methods in Enzymology*, 2015.
20 [8] S. Stoll and A. Schweiger, *J. Magn. Reson.*, **2006**, 178, 1, 42–55.
21 [9] E. Etienne, N. Le Breton, M. Martinho, E. Mileo, and V. Belle, *Magn. Reson. Chem.*, **2017**, 55, 8, 714–719.
22 [10] A. Van Der Est, *eMagRes*, **2016**.
23 [11] C. Duboc, *Chem. Soc. Rev.*, **2016**, 45, 21, 5834–5847.
24 [12] S. Stoll, *Handb. Multifrequency Electron Paramagn. Reson. Data Tech.*, **2014**, 69–138.
25 [13] J. Chen *et al.*, *ACS Catal.*, **2018**, 8, 10, 9665–9674.
26 [14] R. Cammack and C. E. Cooper, *Methods Enzymol.*, **1993**.
27 [15] G. Roelfes *et al.*, *Inorg. Chem.*, **2002**, 38, 8, 1929–1936.
28 [16] A. Draksharapu, Q. Li, G. Roelfes, and W. R. Browne, *Dalt. Trans.*, **2012**, 41, 42, 13180–13190.
29 [17] N. O'Toole *et al.*, *Eur. J. Inorg. Chem.*, **2019**, 2019, 1, 73–78.
30 [18] N. Hall *et al.*, *Inorg. Chem.*, **2016**, 55, 4, 1497–1504.
31 [19] B. J. Hathaway and D. E. Billing, *Coord. Chem. Rev.*, **1970**.
32
33
34
35
36
37
38
39
40
41
42
43
44
45
46
47
48
49
50
51
52
53
54
55
56
57
58
59
60